# White point estimation of an RGBC color sensor to measure dominant wavelength

Rafael A. Ortega-Cohen[1], Hernando Altamar-Mercado[2], Carlos R. Payares-Guevara[3], Enrique Pereira-Batista[4], Cristina Osorio-del-Valle[5], Vilma-Viviana Ojeda-Caicedo[6], Alberto Patiño-Vanegas[7]

[1−7]Facultad de Ciencias Basicas, Universidad Tecnologica de Bolivar, Cartagena de Indias, Colombia.

[1]rortega@utb.edu.co, [2]haltamar@utb.edu.co, [3]cpayares@utb.edu.co,
[4]ebatista@utb.edu.co, [5]cosorio@utb.edu.co,[6]vojeda@utb.edu.co
Corresponding author:[7]apatino@utb.edu.co

***Abstract*—This paper introduces a novel methodology for calibrating an RGBC sensor to estimate the dominant wavelength of visible light sources with high precision and low cost. Unlike traditional approaches, the method accounts for sensor-specific deviations by estimating a customized white point using three quasi-monochromatic filters (405 nm, 546 nm, and 578 nm), enhancing measurement accuracy across the visible spectrum. The calibration procedure includes (i) normalization of the RGB signal using the clear channel (C), (ii) transformation to the CIE 1931 XYZ color space, (iii) mapping to chromaticity coordinates (xyY), and (iv) interpolation within the CIE chromaticity diagram to extract the dominant wavelength. The proposed system employs a TCS34725 sensor with infrared suppression, integrated into a low-cost data acquisition setup based on an ATmega328P microcontroller. Experimental results demonstrate wavelength estimation errors as low as 0.01%, validating the approach as a viable alternative to conventional spectrometers. This method holds significant potential for applications in real-time colorimetric sensing, display calibration, portable spectroscopy, and environmental monitoring, especially in resource-constrained settings.**

***Index Terms*—White Point, RGBC, color sensor, wavelength, chromatic diagram, CIE, color space**

## I. Introduction

RGB sensors have been widely applied in various fields due to their capability of detecting and quantifying color variations with high sensitivity. Some notable applications include rotation angle measurement in non-contact rotary machines, achieving a high resolution of $0.08°$, which is limited by the resolution of the analog-to-digital converter (ADC) [1]; color reproduction in multimedia devices, where improvements have been achieved by measuring RGBC components of ambient light and applying compensation functions to enhance color accuracy [2]; glucose concentration determination in plasma samples using colorimetric analysis [3], [4]; and the quantification of curcuminoids in turmeric, achieving a measurement reliability of 95% [5]. Additionally, RGB sensors have been employed in real-time colorimetric measurements, where they have demonstrated comparable performance to commercial spectrophotometers in detecting and quantifying colored solutions without requiring extensive computational resources [6].

One of the main challenges in using RGB sensors is their sensitivity to ambient radiation and variations in light source intensity. Factors such as background illumination, sensor drift, and exposure settings can introduce errors, affecting the accuracy of colorimetric measurements [7]. To mitigate these issues, recent studies have explored transformation techniques, such as converting RGB values into alternative color spaces like HSV (Hue, Saturation, and Value), which provides a color distribution closer to the spectral characteristics of visible light. Other approaches have focused on calibrating RGB sensors through machine learning models or using additional filtering techniques to enhance measurement reliability in uncontrolled environments [7].

This paper proposes a methodology to calibrate an RGBC sensor for measuring the dominant wavelength of visible light sources. The methodology is based on the use of the TCS34725 sensor, which is capable of blocking infrared components and providing an intensity signal (C), thus enabling an invariant measurement with respect to ambient radiation and light source intensity. The proposed approach employs the CIE XYZ 1931 color space, along with the chromaticity diagram of the CIE xyY color space, assuming that the sensor operates in the standard RGB color space. To enhance accuracy, we suggest using a white light source and three optical filters to obtain three quasi-monochromatic sources, which are used to establish the sensor's white point. The dominant wavelength of incident light is then measured relative to this white point.

This methodology is particularly relevant for applications requiring precise colorimetric analysis, including spectroscopy, environmental sensing, and display calibration. Recent research has demonstrated that RGB-based colorimetric sensors can be successfully applied in real-time analytical chemistry, offering a cost-effective alternative to conventional spectrophotometry [6], [8]. Moreover, studies on CMOS-based RGB image sensors have investigated their hue-wavelength response, highlighting their potential in wavelength determination and optical sensing applications [7].

By addressing the challenges of RGB sensor calibration and improving measurement accuracy, this study contributes to the development of more robust and reliable colorimetric sensing

methodologies.

## II. Materials and color space

The purpose of colorimetry is to relate the physical measurement of light and color perception. In this work we want to estimate the dominant wavelength of a quasi-monochromatic light source from the signal supplied by an RGBC sensor. The data acquisition system and the color spaces used are described below.

### A. Data acquisition system

The data acquisition system is mainly based on an RGBC sensor with a spectral response within the visible range. Such a sensor is connected to a data acquisition card whose function is to read the RGBC signal given by the sensor and then send it to a computer for processing. In this work, we have selected the TCS34725 [9] color sensor, because it provides a digital return of red, green and blue (RGB), and a digital return of incident light intensity (C). In addition, because it has a built-in IR blocking filter integrated in the chip and located in the color sensor photodiodes to minimize the IR component of the incident light spectrum. In Figure 1 it can be seen that the spectral response of the photodiode is comparable to the spectral response of a standard (colorimetric) observer. This type of sensors also facilitates the study of the signal because the photodiodes incorporate a 16-bit Analog/Digital Converter (ADC) [9].

On the other hand, Arduino UNO R3 was chosen as the data acquisition card. The communication of this card with the RGBC sensor is carried out through an $I^2C$ serial bus and with the computer through a serial port controlled by a Universal Asynchronous Transmitter-Receiver (UART) device [10]. Arduino receives the values of the $R$, $G$, $B$ and $C$ signal between 0 and $2^{16} - 1$; and transmits them to the computer (see Fig. 2).

### B. CIE XYZ 1931 color space

The CIE XYZ 1931 color space was established in 1931 by the Commission Internationale de l'Éclairage (CIE), based on a series of experiments carried out in the late 1920s. With this space, the three primary colors of the additive synthesis of Color have been defined precisely. From those primary colors all others can be created. In this model Y means luminosity, Z is approximately equal to the stimulus of blue (cones S), and X is a mixture tending to the sensitivity curve from red to green (cones L and M). In this way, XYZ can be confused with the responses of cones in RGB. However, in the CIE XYZ color space, triple stimulus values do not equal the S, M and L responses of the human eye, even considering that X and Z are approximately red and blue, as can be seen in figure 1(b). Actually, they should be seen as "derived" parameters of the colors red, green and blue .

### C. The CIE xy chromaticity diagram

The CIE xyY space was deliberately designed, such that the $Y$ parameter is a measure of the brightness or luminosity of a color. The chromaticity of a color is then determined through two parameters derived $x$ and $y$, normalized according to the three values $X$, $Y$ and $Z$:

$$x = \frac{X}{X+Y+Z} \tag{1}$$

$$y = \frac{Y}{X+Y+Z} \tag{2}$$

Figure 3 shows the chromaticity diagram related to the $xy$ coordinates. Mathematically, $x$ and $y$ are projection coordinates and the colors of the chromaticity diagram are part of a region of the projection plane. The curved outer boundary is the spectral niche, whose wavelengths are shown in nanometers. The diagram represents all the chromaticities visible by an average person. These are shown in color, and this region is known as the range of human vision. In the spectral niche each point represents a pure hue of a single wavelength. The less saturated colors appear inside the scheme, with the white point towards the center.

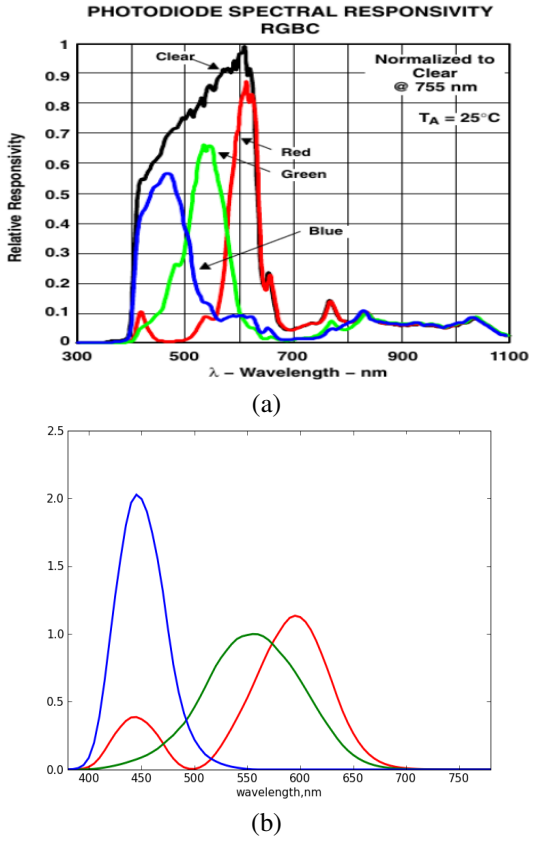


Fig. 1. (a) Photodiode spectral responsivity (RGBC), (b) CIE 1931 XYZ Color Matching Functions. (Adapted from https://en.wikipedia.org/wiki/CIE_1931_color_space)

### D. RGB standard color space (sRGB)

sRGB or RGB standard defines red ($R$), green ($G$) and blue ($B$) as primary colors. In the $xy$ chromatic coordinates defined by the equations 1 and 2, the primary red is $(0.6400, 0.3300)$,

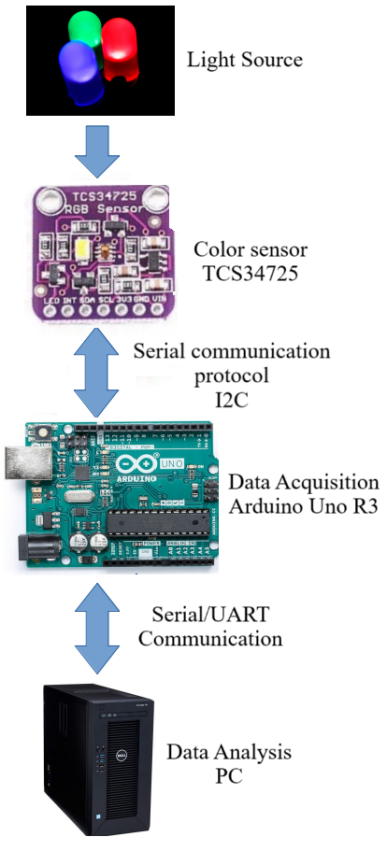


Fig. 2. Data acquisition system

the primary green is $(0.3000, 0.6000)$ y the primary blue in $(0.1500, 0.0600)$. The white point (D65) is located at the coordinates $(0.3127, 0.3290)$. The rest of the colors are produced with a linear combination of the primary colors. To convert the triestimulus values R, G and B of the sRGB color space to the $X$, $Y$ and $Z$ coordinates of the CIE XYZ 1931 color space, the following transformation is performed:

$$\begin{bmatrix} X \\ Y \\ Z \end{bmatrix} = \begin{bmatrix} 0.412424 & 0.357579 & 0.180464 \\ 0.212656 & 0.715158 & 0.072186 \\ 0.019332 & 0.119193 & 0.950444 \end{bmatrix} \begin{bmatrix} g(R) \\ g(G) \\ g(B) \end{bmatrix} \quad (3)$$

with

$$g(K) = \begin{cases} \left(\frac{K+a}{1+a}\right)^{\gamma} & \text{for all } K > 0.04045 \\ \frac{K}{\phi} & \text{otherwise} \end{cases}$$

Here, $K$ represents any value $R$, $G$ or $B$ normalized in the range of 0 to 1.

### *E. Relationship between xy coordinates and wavelength*

We reason according to figure 3. Suppose we want to obtain the dominant wavelength from the point represented by an "$\times$" with chromatic coordinates $(x, y)$ in the sRGB color space. We know that any point in the chromatic diagram on a line

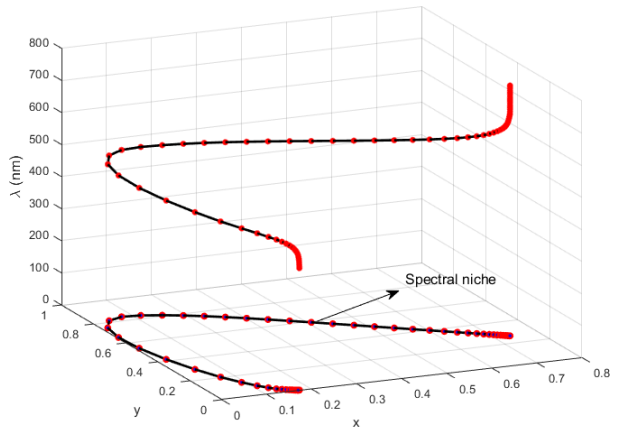


(a)

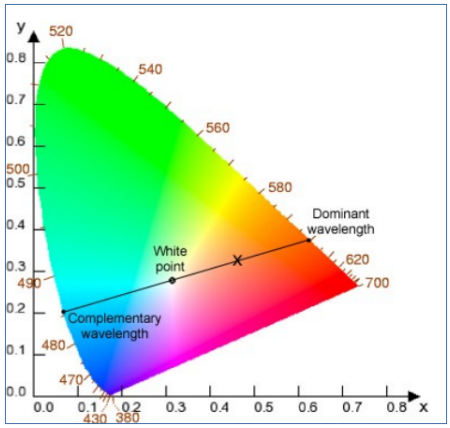


(b)

Fig. 3. (a) $\lambda = f(x, y)$, $(x, y) \in$ espectral niche, (b) CIE xyY chromaticity diagram (Adapted from https://en.wikipedia.org/wiki/CIE_1931_color_space).

that passes through the white point D65 will have the same chromaticity. With this, we draw a line that joins the point "$\times$" with the point D65. The value of the corresponding wavelength is the point of intersection of such a line with the spectral niche. The point of intersection closest to the point "$\times$" is defined as the dominant wavelength and the geometrically opposite intersection is defined as complementary wavelength.

## III. Method

To estimate the dominant wavelength of a quasi-monochromatic light source from the $R$, $G$, $B$ and $C$ signal recorded by the sensor, we propose the following procedure (see Fig. 4 ):

i. Normalization of the $RGB$ signal between 0 and 1. Although the maximum digital value that each sensor can provide is $V_{max} = 2^{16} - 1$, each value $RGB$ could be divided by $V_{max}$ to normalize them between 0 and 1. We prefer to normalize the $RGB$ values for their corresponding $C$ value since this value is proportional to the total intensity of the source at the time of registration

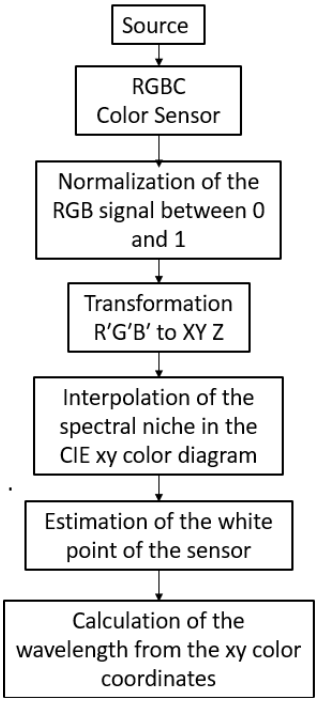


Fig. 4. Flowchart to illustrate the procedure to obtain the dominant wavelength of the quasi-monochromatic source

and reaches the maximum possible values within the operating spectrum. This ensures that the estimate of the wavelength is invariant to the intensity of the source. Then, the normalized values in the range of 0 to 1 are obtained as follows:

$$K' = \frac{K}{C}, \tag{4}$$

where $K$ is any of the $R$, $G$ or $B$ values recorded by the sensor and $K'$ is the respective normalized RGB component value.

ii. Transformation $R'G'B'$ to $XYZ$. Here we initially assume that any standard triplet $(R', G, B')$ given by the sensor belongs to the sRGB color space, as can be seen in figure 1. Then, to perform the transformation of the $R'$, $G'$ and $B'$ values given by the sensor to the CIE XYZ color space, the equation 3 is used. The normalized values $R'G'B'$ were calculated with the equation (4). The values $a = 0.055$, $\phi = 12.9232$ and $\gamma = 2.4$ recommended by IEC 61966 have been used.

iii. Interpolation of the spectral niche in the CIE xy color diagram. In the curve of the spectral niche there are the values of the wavelengths every 5 nm and their corresponding coordinate $(x, y)$. To obtain a better accuracy in the measurement of the dominant wavelength, we have performed an interpolation of the chromatic diagram. For this, we have made an interpolation of the function $\lambda = f(x, y)$ ($x, y$ belong to the spectral niche) and then we have made a projection on the plane $xy$. Thus, we have obtained values less than 5 nm between adjacent points of the spectral niche, improving the resolution.

iv. Estimation of the white point of the sensor. We have used a monochromatic source of known wavelength and have calculated the point $(x, y)$ obtained from the values $R'$, $G'$ and $B'$ given by the sensor. Then, we have drawn a line that has passed through the point $(x, y)$ and the corresponding wavelength value in the spectral niche and we have observed that such line does not pass through point D65. Then, the initial assumption that the RGB values given by the sensor belong to the sRGB space is not true and we must make a correction. We propose recalculate the coordinates of the white point for the sensor used. For this, we have used three monochromatic sources of very narrow spectrum and the three corresponding lines have been represented in the chromatic diagram. Then, the chromatic coordinates of the centroid of the triangle that form the three lines have been calculated. The coordinates of such centroid are the ones we have used as the white point of the sensor.

v. Calculation of the wavelength from the xy color coordinates. It was performed with the procedure described in the section II-E, using the chromatic coordinates of the white point obtained from the sensor used.

## IV. Results and Discussion

### A. White point calculation of the sensorr

To obtain the white point of the sensor 3 interference filters for wavelengths of 405 nm, 546 nm and 578 nm were used. The interference filters were placed in front of a white light source before the light hit the sensor. Figure 5 shows the spectrum recorded with each of the three filters using a calibrated Ocean Optics USB spectrometer. This USB Spectrometer covers the visible, UV and near IR ranges of the electromagnetic spectrum.

The white point of the sensor was calculated following the procedure described in section III(iv). The lines obtained for each known wavelength and the white point (marked with *) are shown in figure 6. The white point coordinate of the calculated sensor was Ds$(0.3435, 0.3704)$. We can observe the appreciable difference in the location of the white point of the sensor and the white point D65. This indicates that each sensor has its own white point Ds.

This result validates the necessity of sensor-specific white point calibration, as assuming a universal D65 white point leads to systematic wavelength estimation errors.

### B. Measurement of the dominant wavelength

To validate the accuracy of the system, 9 quasi-chromatic LED sources were used. The RGBC values provided by the sensor for each source were recorded for each source.

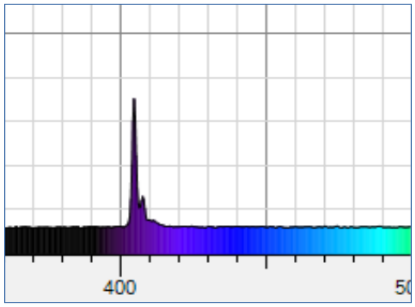


(a) 405nm

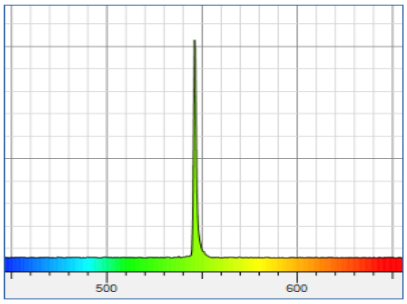


(b) 546nm

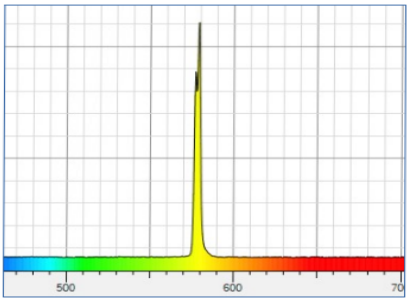


(c) 578nm

Fig. 5. Wavelengths used to obtain the chromatic coordinates of the white point of the sensor

Wavelengths were calculated using the procedure described in section III. Figure 7 shows the results obtained for the $(x, y)$ coordinates in the sRGB color space for each of the sources used in the methodology validation process. Table I shows the light sources used with their respective wavelength measured with the calibrated Ocean Optics USB spectrometer, the respective dominant wavelength measured with the RGBC sensor and the relative error. It can be seen that the greatest errors are found when the source has a wavelength at the end of the chromatic niche close to 400 nm (405 and 464 nm). This behavior is attributed to the high gradient and point density in that region of the chromaticity diagram, where small chromaticity shifts produce substantial wavelength deviations. In contrast, wavelengths closer to the center of the diagram, such as 546 nm and 578 nm, exhibited excellent agreement with spectrometer readings, with errors as low as 0.02%.

Compared to previous studies, such as Oliveira et al. [6], who reported typical errors in the 3–7% range for RGB-based colorimetric systems without white point correction, our method shows a marked improvement. Additionally, Park et al. [7] noted that conventional RGB sensor readings tend to cluster around standard white points, often introducing consistent chromatic bias. Our use of sensor-specific white point estimation directly addresses this limitation, leading to increased precision and lower variance in wavelength estimation.

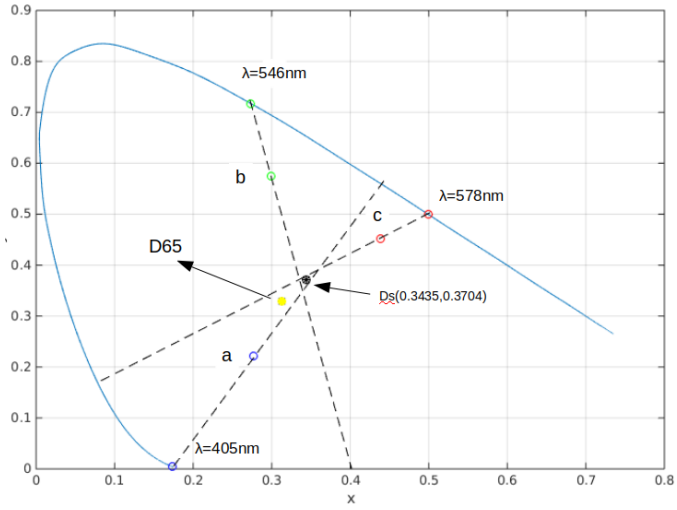


Fig. 6. Location of the white point of the sensor Ds compared to the white point D65

TABLE I
DOMINANT WAVELENGTH MEASURED BY THE SENSOR AND ITS RESPECTIVE ERROR RELATIVE TO THE WAVELENGTH OF THE SOURCE

| Source-$\lambda$ (nm) | Sensor-$\lambda$ (nm) | Error(%) |
|---|---|---|
| 467.97 | 465.67 | 0.48 |
| 575.40 | 557.87 | 3.05 |
| 590.00 | 602.52 | 2.12 |
| 608.30 | 613.81 | 0.91 |
| 405.00 | 385.04 | 4.93 |
| 436.00 | 464.79 | 6.60 |
| 546.00 | 545.28 | 0.13 |
| 578.00 | 577.90 | 0.02 |
| 632.80 | 620.56 | 1.93 |

Figure 8 illustrates the correlation between the spectrometer-measured and sensor-estimated wavelengths, highlighting the method's validity across the spectrum. Notably, even in spectral regions prone to error, such as near 400 nm, the estimation remains within acceptable margins for most practical applications.

The selection of the 405 nm, 546 nm, and 578 nm interference filters was strategically made to span distinct regions of the visible spectrum—violet, green, and yellow-orange—providing sufficient chromatic diversity to accurately estimate the sensor's white point through triangulation in the chromaticity diagram. This configuration ensures a robust geometric calibration, independent of assumptions tied to standard sRGB behavior. Additionally, environmental variability, such as fluctuations in ambient illumination or source intensity, was

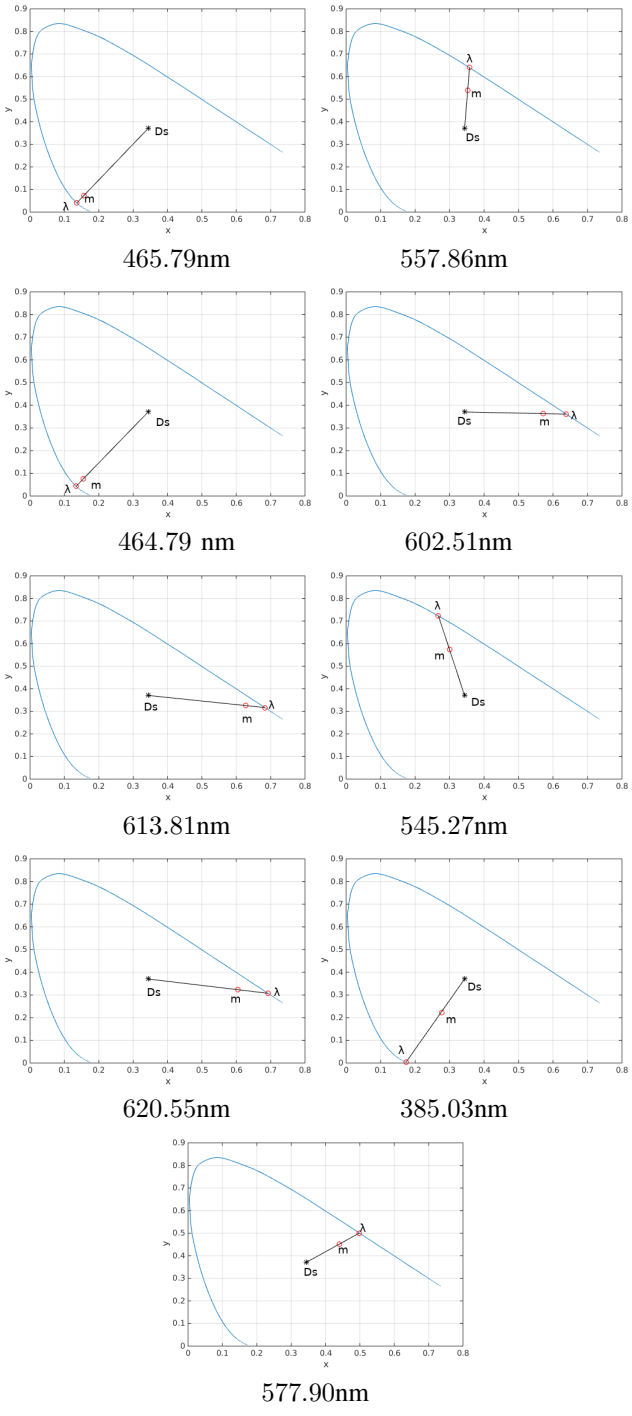


Fig. 7. Procedure performed for the calculation of the dominate wavelength of different quasi-chromatic sources

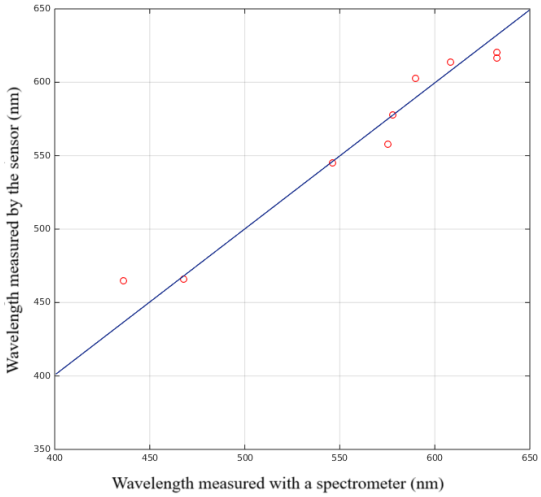


Fig. 8. Comparison of the wavelength measured with a spectrometer and the one measured with our method using an RGBC sensor

mitigated by normalizing the RGB values using the Clear (C) channel. This normalization renders the measurement process invariant to absolute intensity, thereby enhancing the reliability and repeatability of the method under varying lighting conditions.

## V. Conclusions

This study presented a robust methodology for estimating the dominant wavelength of quasi-monochromatic light sources using an RGBC sensor in conjunction with the CIE XYZ and sRGB color spaces. The main contribution lies in the normalization of the RGB components with respect to the Clear (C) signal, enabling intensity-invariant measurements and reducing the influence of ambient radiation.

An innovative procedure was also proposed for determining the sensor-specific white point by employing three optical filters with known wavelengths. This calibration corrected for the deviation from the standard D65 white point and significantly improved the accuracy in dominant wavelength estimation, yielding relative errors ranging from 0.01% to 6.6%. The highest errors were observed in the spectral region near 400 nm, where small variations in chromatic coordinates result in substantial deviations in wavelength estimation due to the high density of interpolated points in that area of the chromaticity diagram.

The proposed methodology demonstrates that accurate spectral estimation can be achieved without the need for high-end spectrometers, paving the way for low-cost applications in colorimetry, optical sensing, and embedded systems for spectral analysis.

Future work will explore the integration of deep learning models for real-time adaptive calibration, as well as the extension of the method to CMOS sensors and more complex lighting environments, thereby broadening its applicability in industrial, biomedical, and environmental monitoring contexts.

## REFERENCES


[1] Kwon Y and Kim W 2014 *IEEE/ASME Transactions on Mechatronics* **19** 1707–1715 ISSN 1083-4435

[2] Eung-Joo Lee, In-Gab Jeong, Yang-Woo Park, Yeong-Ho Ha and Gwang-Choon Lee 1996 *IEEE Transactions on Consumer Electronics* **42** 182–191 ISSN 0098-3063

[3] Sivanantha Raja A and Sankaranarayanan K 2007 Performance analysis of a colorimeter designed with rgb color sensor *2007 International Conference on Intelligent and Advanced Systems* pp 305–310

[4] Mello M M, Lincoln V A C, Barcellos R, Cirino G A, Schiabel H and Ventura L 2019 A new method for estimating photometric and colorimetric properties using RGB sensor and ANN *Physics, Simulation, and Photonic Engineering of Photovoltaic Devices VIII* vol 10913 ed Freundlich A, Lombez L and Sugiyama M International Society for Optics and Photonics (SPIE) p 109131I URL https://doi.org/10.1117/12.2510397

[5] Supannarach S and Thanapatay D 2008 The study of using rgb color sensor to measure the curcuminiods amount in turmeric (curcuma longa linn.) and zedoary (curcuma zedoarie rose.) by comparing colors with hsl system *2008 5th International Conference on Electrical Engineering/Electronics, Computer, Telecommunications and Information Technology* vol 1 pp 529–532

[6] Oliveira G d C, Machado C C S, Inácio D K, Petruci J F d S and Silva S G 2022 *Talanta* **241** 123244 URL https://doi.org/10.1016/j.talanta.2022.123244

[7] Park H W, Choi J W, Choi J Y, Joo K K and Kim N R 2022 *Sensors* **22** 9497 URL https://doi.org/10.3390/s22239497

[8] Cha E and Lee H 2024 *Journal of International Research in Medical and Pharmaceutical Sciences* **19** 24–36 URL https://ikprress.org/index.php/JIRMEPS/article/view/8608

[9] TAOS Texas Advanced Optoelectronic Solutions Inc 2012 *TCS3472 Color Light-To-Digital Converter With Ir Filter* URL www.taosinc.com

[10] ATMEL *8-bit AVR Microcontroller with 4/8/16/32K Bytes In-System Programmable Flash*